Pergamon

Journal of Structural Geology, Vol. 17, No. 5, pp. 607 to 614, 1995

0191-8141/95 $9.50 + 0.00

0191-8141(94)00091-3

Displacement-length scaling and fault linkage

NANCYE H. DAWERS and MARK H. ANDERS

Lamont-Doherty Earth Observatory and Department of Geological Sciences, Columbia University, Palisades, NY 10964, U.S.A.

(*Received* 9 *March* 1994; *accepted in revised form* 2 *August* 1994)

Abstract—Large fault systems often result from the linkage of smaller faults. This produces an increase in fault length, but a deviation from the simple displacement pattern observed for individual faults. Here we examine the displacement distribution along a ~7 km long normal fault system composed of overlapping segments, and numerous small splays and non-intersecting subparallel faults. The absence of appreciable sedimentation or erosion associated with this young (<765 ka) fault system allows us to accurately map throw along it. Our results show that the scaling relationship obtained previously for single-segment faults of the same fault population is generally applicable to the fault system described here, if the throw is assessed by adding displacements that occur between segments. We suggest that the smaller faults grew during and after the coalescence of the larger fault segments in order to release large strains in the regions of linkage, thereby maintaining the scaling relationship throughout the growth of the fault system. Although this study was carried out on a relatively small normal fault system, we believe this pattern of fault growth is applicable to all scales as well as to strike-slip and thrust systems.

INTRODUCTION

Studies of brittle fault populations show that fault growth is governed by a scaling relationship between displacement (D) and length (L), such that $D \propto L^n$. Attempts to characterize n concluded $n = 2$ (Watterson 1986, Walsh & Watterson 1988) or $n = 1.5$ (Marrett & Allmendinger 1991, Gillespie *et al.* 1992), but subsequent interpretation (Cowie & Scholz 1992a) and more recently acquired data indicate $n = 1$ (Gudmundsson 1992, Dawers *et al.* 1993). The physical basis for this has been explained by Cowie & Scholz (1992b), but their model, as well as previously proposed models, assumes that faults can be viewed as simple, isolated cracks. Many studies, however, have convincingly shown that fault growth by the coalescence and linkage of smaller faults is common (e.g. Segall & Pollard 1983, Granier 1985, Ellis & Dunlap 1988, Martel *et al.* 1988, Peacock & Sanderson 1991, 1994, Anders & Schlische 1994, Trudgill & Cartwright 1994, Cartwright *et al.* personal communication). During the initial stage of fault coalescence, a linked fault's length is the sum of the lengths of the smaller faults or fault segments, while the maximum displacement remains the greatest value of the smaller faults (Fig. 1). In order for any of the proposed scaling relationships to be generally applicable, significant displacement must be accommodated in regions of linkage and also accumulate within the central portion of fault zone (Anders *et al.* 1992).

Data provided by Walsh & Watterson (1990, 1991) and Peacock & Sanderson (1991) suggest that segmented faults have a ratio of cumulative displacement (D) to length (L) consistent with the total length of the array, rather than that expected for the segment length. Here we discuss the displacement pattern observed along a fault having a complex surface trace, which we attribute to growth of the fault by coalescence of en échelon fault segments. We have previously discussed the D–L relationship observed for relatively simple, single-segment faults occurring at the same locality (Dawers *et al.* 1993). The data from this linked, en échelon array indicate that the observed D–L relationship for single faults is also applicable to more complex faults formed by linkage.

STUDY AREA

The study area is located on the Volcanic Tableland of northern Owens Valley, California (Fig. 2). Owens Valley is a NNW-trending valley that lies at the western margin of the Basin and Range Province, in a region characterized by both strike-slip and normal faulting. In northern Owens Valley geodetic and geologic data indicate ~EW extension (e.g. Savage *et al.* 1981,

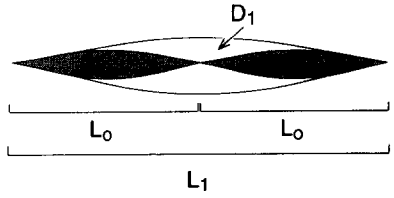

Fig. 1. A schematic illustration of the linkage of two fault segments of length L_0. Initially the total fault zone length is $2L_0$, but the maximum displacement is approximately that of earlier formed segments, D_0. If larger faults that result from the linkage of smaller faults are to exhibit displacement-length scaling of the form, $D \propto L^n$, where n is either 2 (Watterson 1986, Walsh & Watterson 1988), 1.5 (Marrett & Allmendinger 1991), or 1 (Cowie & Scholz 1992a,b), then displacement of at least D_1 must be accommodated within the region of linkage.

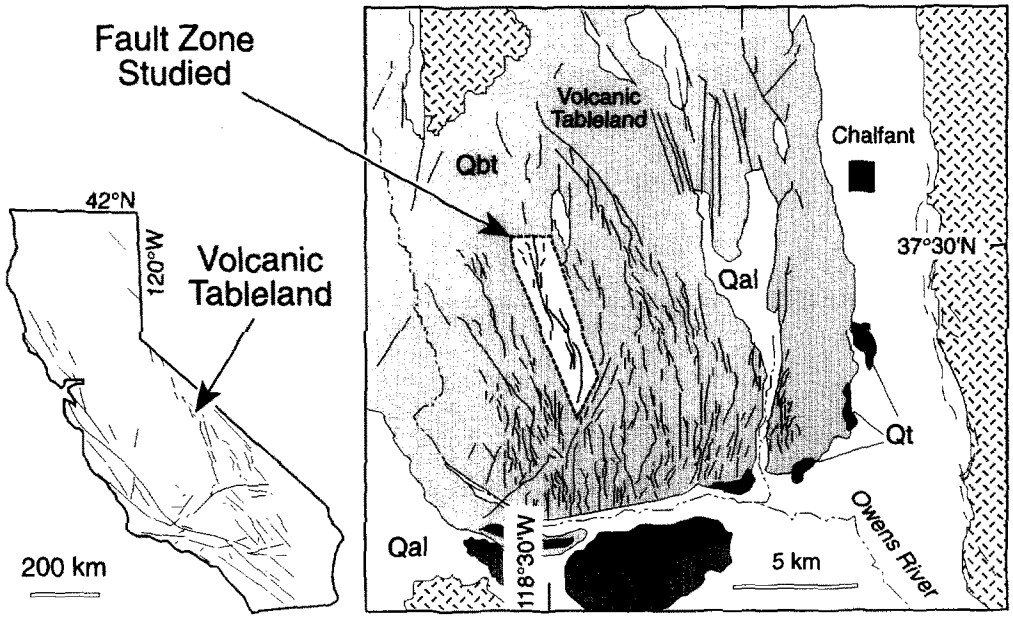

Fig. 2. Location of the fault zone on the Volcanic Tableland, in eastern California. Qbt = Bishop Tuff; Qt—terrace deposits, undivided; Qal—alluvium, undivided. Cross-hatched pattern = upper Precambrian through Tertiary rocks, undivided. Map modified from Strand (1967).

Pinter 1992, respectively), in contrast to central and southern Owens Valley, where the extension is ~NW–SE and faults parallel to the valley experience a greater component of right-lateral shear (e.g. Savage *et al.* 1981, Lubetkin & Clark 1988).

The Volcanic Tableland itself is a topographic plateau formed by the Pleistocene Bishop Tuff. The Bishop Tuff varies regionally in thickness and in the degree of welding (Gilbert 1938, Bateman 1965). On average the thickness is estimated to be between about 120 and 150 m (Gilbert 1938). In the area of interest here, i.e. the highly faulted region of the Tableland shown in Fig. 2, exposed sections suggest that the thickness is ~80–150 m. Here Bateman (1965) mapped the tuff as 'agglutinated', because the consolidation of the tuff is due primarily to growth of crystallites, rather than compaction and welding. Along the extreme southern and eastern margins of the Tableland the tuff is thinner, and the lower portion of the tuff is soft and poorly consolidated. Underlying the tuff sheet is unconsolidated airfall ash and older alluvial sediments of undetermined thickness. Because of the apparent low competency of the basal portion of the tuff and the underlying sediments, we speculate that the faults in this locality may have nucleated in the more competent upper portion of the tuff. Several lines of evidence discussed in Dawers *et al.* (1993) are consistent fault nucleation in the near-surface. We note, however, that this may not be the case for faults in thicker sections where the tuff is truly welded, and possibly stronger, near the base (Gilbert 1938, Bateman 1965).

The fault zone discussed here is one of many N-striking normal faults that offset the tuff at this locality (Bateman 1965, Sheridan 1975, Pinter 1992) (Fig. 2). The fault zone extends for >7 km, forming a series of prominent topographic breaks that result from displacement of the erosionally-resistant, and predominantly horizontal, upper surface of the Bishop Tuff (Fig. 3). The lack of significant erosion (Gilbert 1938) or deposition since the emplacement of the 765±5 ka (Izett & Obradovich 1994) ash-flow sheet allows scarp height to be used as an accurate measure of total throw (see Bateman 1965, Dawers *et al.* 1993).

FAULT ZONE GEOMETRY

The fault zone consists of four main, left-stepping en échelon fault segments that range in length from 1530 to 2563 m (Figs. 3 and 4a). The largest throw (~90 m) occurs near the center of the fault zone, on the shortest of the four main fault segments. Between the overlapping fault segments are tilted regions, or relay ramps, that connect the footwall of one segment to the hanging-wall of an overlapping segment (Larsen 1988, Peacock & Sanderson 1991). The relay ramps are broken by numerous subparallel faults and small splays. At the northern end of the fault zone, the displacement is distributed on a number of splaying faults. The strike-slip component on the principal fault segments is inferred to be insignificant. This inference is based on the lack of observable lateral offset of an abandoned stream channel near the center of the fault zone (Figs. 3 and 4a). We estimate the bedrock scarps to dip at an angle >30°, but because of the uncertainty in the dip of the scarps, throw is used here as a proxy for displacement.

Throw vs. distance

The throw was determined by measuring the change in elevation across the four main fault segments, as well as the smaller, discrete fault segments within the relay ramps and in the splaying zone (Fig. 4), using a total-station surveying instrument. Segment length, as used

Fig. 3. Aerial photo of the fault zone. The sun angle is from the west, producing shadows on the E-facing scarps. The fault zone studied is the left-stepping array that occupies most of the central portion of the photo. The area shown is roughly 4 × 8 km. Arrows indicate an abandoned stream channel that crosses several large fault segments without evidence of lateral offset; this indicates fault movement is predominantly normal.

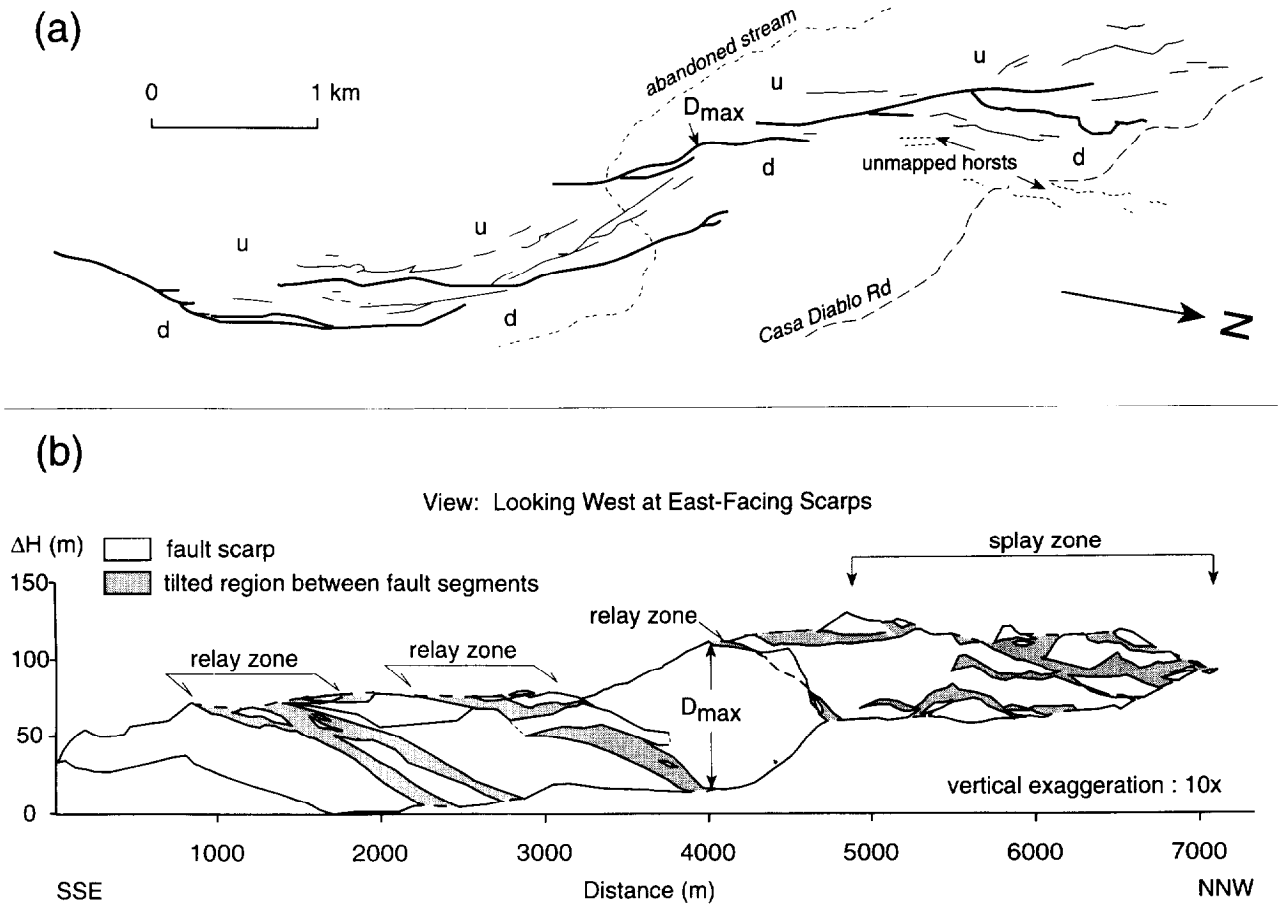

Fig. 4. (a) Map view of the mapped fault segments. (b) Elevation change along the strike of the fault zone; the view is looking toward the scarps from the hangingwall. The shaded regions represent tilting of the upper surface of the tuff toward the hangingwall. Note that smaller faults are concentrated at the overlapping regions of the four large throw segments and in the splay zone at the northern fault tip.

here, is the distance measured along a continuously exposed fault scarp, between the segment tips at which scarp height has diminished to zero. For the fault zone studied here, we found that in most cases segment length can be objectively characterized in this way. A notable exception to this is the NW-striking fault segment that directly links the two central main segments (Figs. 2 and 4a). The length of this fault segment is taken to be the distance between its intersection points with the two main segments. Note also that Fig. 4(a) shows that several fault segments splay. We do not attempt to further subdivide such cases, i.e. for a segment that splays, the length and throw reported in Figs. 4, 5 and 6 are aggregate values.

We mapped 31, E-facing fault segments that are ≥40 m in length. We estimate that the accuracy of our throw measurements is ±1 m; this uncertainty is due to small-scale irregularities on the surface, and slope-wash debris and aeolian sand deposited at the bases of the larger scarps. We decided in the field to omit faults that bound a few small horsts; although these structures contribute to extension, there is some uncertainty as to how they are related to the E-facing fault array. Our aim here is to discuss the salient features of the fault zone, and alternative interpretations of these and other small faults would not significantly change the conclusions of this paper.

In Fig. 4(b) we show the along-strike throw of the top of the Bishop Tuff, projected onto a vertical plane parallel to the main segments; i.e. the variation in elevation difference as viewed normal to the scarps from the hangingwall. From Fig. 4(b) several observations can be made: (1) the total throw tapers to zero at tips of the fault zone; (2) the regions where the principal fault segments overlap do not contain large deficits in total throw, suggesting that deformation is accommodated by faulting and by tilting of the relay zones toward the hangingwall; and (3) much of the deformation in the splay zone results from such tilting.

The throw vs. distance along the fault zone is shown in Fig. 5. The four main segments are clear because of the large throws (>40 m) that occur along them. We also show two summed profiles in Fig. 5: (1) the summed throws on all of the mapped scarps, and (2) the total throw profile. The total throw includes that component of the deformation related to tilting in the relay zones and in the splay zone, i.e. the shaded area of Fig. 4(b) or the component of deformation which (at the scale of our observations) can be considered 'continuous'. Also shown for reference is the region in which we expect throw vs. distance data for a single-segment fault of L=7130 m to plot (Fig. 5); this is based on single-segment data of Dawers *et al.* (1993).

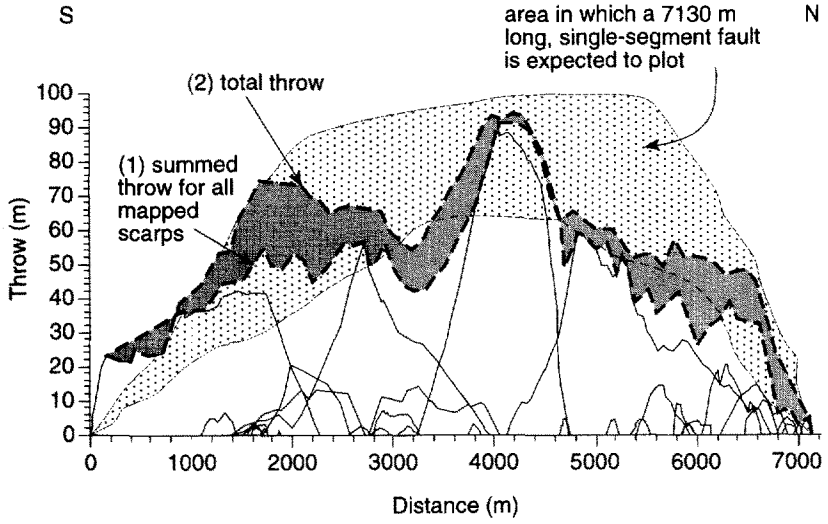

Fig. 5. Throw vs. distance. The four main segments are clear from the large throws (>40 m). Also shown is (1) a summed throw profile, which is constructed by summing the throws measured on all of the mapped scarps; and (2) a total throw profile, which includes the elevation change related to 'continuous' deformation (i.e. tilting between fault segments, as well as any unmapped small faults). The shaded region below the total profile represents the shaded region in Fig. 4(b). The stippled region represents the area in which we expect throw vs. distance data for a single-segment fault of L = 7130 m to plot, based on observations of single-segment faults on the Tableland reported in Dawers *et al.* (1993). This region is derived by enveloping the spread of data points for their length-normalized throw-vs.-distance data, using faults that are appropriate for comparison here—those of L much greater than the thickness of the Bishop Tuff—and then scaling the region to L = 7130 m [see fig. 2 and discussion in Dawers *et al.* (1993)].

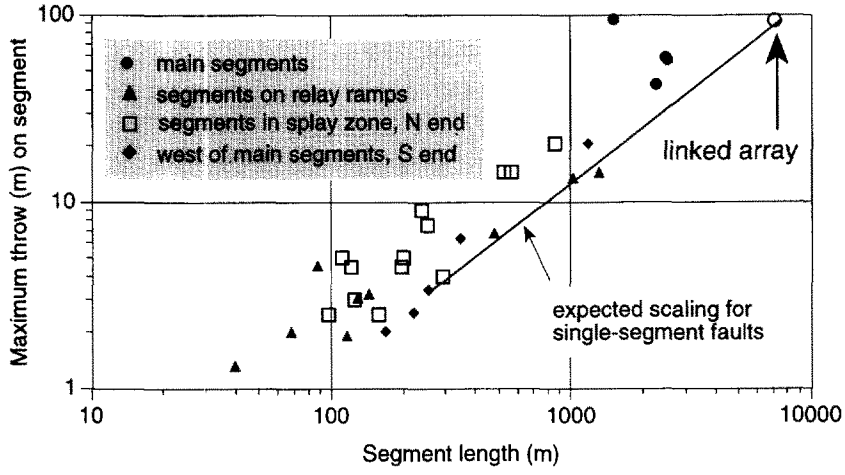

Fig. 6. Maximum throw on segment vs. segment length. The line represents the D_{max} vs. L scaling using the single-segment data (see Dawers *et al.* 1993 for a discussion). Note that the data point for the entire linked array falls along this line, whereas the data for fault segments, if plotted individually, generally lie above the expected scaling for single-segment faults. Following Peacock & Sanderson (1991), we interpret this as the result of displacement transfer across relay structures, which is associated with steep displacement gradients at segment tips, which in turn produces higher D_{max}/L ratios.

Scaling

For single-segment faults on the Volcanic Tableland that are inferred to break through the Bishop Tuff layer, or those having lengths greater than a few times the layer thickness, D is linearly related to L by $D_{max} \sim(0.009–0.014)L$ and $D_{avg} \sim 0.008L$ (Dawers *et al.* 1993). The ratio D_{max}/L for the whole fault discussed here is ~0.013, which is consistent with single-segment faults. The average throw can be estimated for both of the summed profiles shown in Fig. 5 by estimating the areas under the curves and dividing by the total length. Summing throws on the mapped scarps, i.e. the mapped discontinuities, yields an estimate of D_{avg}/L ~0.006, which is less than that of single-segment faults. However, if the 'continuous' deformation is added to the measured fault throws, the ratio D_{avg}/L ~0.008, which is the same as that found for single-segment faults. Scaling ratios for fault segments within the linked fault zone are either similar to previously reported data for single-segment faults, or greater than those previously reported (Dawers *et al.* 1993) (Fig. 6). High D_{max}/L

values tend to be associated with faults located in the splay zone at the northern tip and between the main overlapping segments (Fig. 6).

DISCUSSION AND CONCLUSIONS

Along-strike displacement patterns of segmented normal faults typically depart from those observed for single-segment faults and those predicted from fault growth models, in that local displacement minima often occur at or near the overlapping segment tips (Peacock & Sanderson 1991, 1994). The data presented here show that summing the displacements in the relay regions reduces this deficit, and that adding the continuous deformation related to tilting between segments further reduces the deficit and produces a smoother profile (see also Walsh & Watterson 1989, 1990, 1991). Although the shape of the total displacement profile for this fault zone deviates from that expected for the single-segment data discussed in Dawers *et al.* (1993) (Fig. 5), we emphasize that the *D–L* scaling for the whole zone is consistent with the single-segment data. This suggests that the segmented fault zone essentially acts as a single fault.

The structure of this fault is similar to small normal faults (~10's of meters in length) described by Peacock & Sanderson (1991, 1994), as well as intermediate (Trudgill & Cartwright 1994, Cartwright *et al.* personal communication) and large normal faults (e.g. Gawthorpe & Hurst 1993, Anders & Schlische 1994, Peacock & Sanderson 1994). Peacock & Sanderson (1991) proposed a model of fault growth beginning with the nucleation of non-overlapping faults; as the faults grow longer and overlap, a relay ramp develops, which then becomes faulted and the initially independent faults eventually link to form a larger fault. Their model suggests that the final displacement profile is a proxy for the growth history of the fault. In other words, the location of maximum displacement represents the point of nucleation. Furthermore, this suggests faults with symmetric profiles represent faults that propagated equi-dimensionally from the nucleation point, and that steep displacement gradients and asymmetric profiles result from interactions between faults. Although this pattern of fault growth is a reasonable *a priori* assumption, neither this study nor similar studies (e.g. Peacock & Sanderson 1991, 1994) can unequivocally establish a growth history. However, this assumed pattern of growth is supported by Anders & Schlische's (1994) study of several large normal fault zones where the temporal evolution of the fault segments is better constrained. They used dated stratigraphic horizons to constrain the temporal and spatial pattern of footwall uplift and hangingwall subsidence, and proposed a similar fault growth model. In the Triassic Newark basin, they found that the oldest syn-tectonic sediments correlated spatially with the location of greatest displacement on individual fault segments. For Tertiary Basin and Range Province faults, they found that older, along-strike subbasins exhibited localized maxima in the tilting of older, syn-tectonic units, whereas younger units exhibit a tilt maximum near the center of the whole fault system and the tilt angle tapers off to zero at the tips of the fault zone.

Anders & Schlische's (1994) study indicates that large normal fault zones can grow by a process of independent nucleation, followed by linkage and growth of smaller faults to accommodate strain in the region of linkage, and thereby maintain the observed scaling relationships for the entire fault system. Again, because of the absence of basin-fill deposits of known chronology, our results can only show the final disposition of total displacement, not the timing of how it accrued. We therefore infer a growth history for the Volcanic Tableland faults based on analogy with the observed growth history of larger faults, such as those studied by Anders & Schlische (1994), where the developmental patterns can be documented.

For the fault zone discussed here we infer a developmental sequence beginning with the formation of four main segments as initially independent faults. As the segments propagated toward one another, growth began to be affected by interactions between the faults, leading to the development of relay ramps, and anomalous displacement gradients and high D_{max}/L values (see Peacock & Sanderson 1991, 1994). As the segments grew, the regions of inelastic deformation surrounding the fault tips also grew (Cowie & Scholz 1991b). When the faults reached lengths at which the inelastic regions coalesced, significant deformation began affecting the echelon steps, forming relay ramps. The details of this would have depended on the size and shape of the inelastic zones, as well as the separation of the initial fault segments (Segall & Pollard 1980). As displacement accrued along the central portions of the fault zone, the relay ramps formed were eventually faulted. The lack of local displacement minima in two of the three main relay zones, suggests that the linkage is essentially complete. An apparent displacement deficit in the relay zone south of the maximum displacement (located at ~3200 m from the southern tip) suggests less advanced linkage there (Fig. 5), which may be related to the greater separation between the segments (Figs. 3 and 4a).

In conclusion, we note that segmented thrusts and strike-slip faults share many of the characteristics discussed here (e.g. Ellis & Dunlap 1988, Peacock 1991, respectively). This suggests this pattern of fault growth by linkage is an important process in the development of fault systems. The wide range of scales documented in previous studies suggest that linkage is significant at all scales as well. From the data presented here we conclude that the observed *D–L* scaling relationship, which is conceptually related to isolated faults, is also applicable to faults formed by linkage and can shed light on the growth of segmented faults.

Acknowledgements—We thank Leigh Schaffler, Devin and Philip Bowles for their assistance in the field. Leigh Schaffler did most of the work in assembling the data for the southern half of the fault. Janice Aitchison's assistance with Fig. 3 is much appreciated. This manuscript

was improved by critical reviews by Trenton Cladouhos and Randall Marrett, and comments from John Byrd, Patience Cowie and Steven Wojtal. This work was funded by Sigma Xi, The Scientific Research Society; Exxon Production Research; American Chemical Society grant PRF-24563; and National Science Foundation grants EAR-91-17300 and EAR-93-05175. This is LDEO contribution no. 5243.

REFERENCES

Anders, M. H., Dawers, N. H. & Schaffler, L. E. 1992. Growth and linkage of normal faults. *Geol. Soc. Am. Abs w Prog.* **24**, A156.

Anders, M. H. & Schlische, R. W. 1994. Overlapping faults, intrabasin highs, and the growth of normal faults. *J. Geol.* **102**, 165–180.

Bateman, P. C. 1965. Geology and tungsten mineralization of the Bishop district, California. *Prof. Pap. U.S. geol. Surv.* **470**.

Cowie, P. A. & Scholz, C. H. 1992a. Displacement-length scaling relationship for faults: data synthesis and discussion. *J. Struct. Geol.* **14**, 1149–1156.

Cowie, P. A. & Scholz, C. H. 1992b. Physical explanation for the displacement-length relationship of faults using a post-field fracture mechanics model. *J. Struct. Geol.* **14**, 1133–1148.

Dawers, N. H., Anders, M. H. & Scholz, C. H. 1993. Growth of normal faults: displacement-length scaling. *Geology* **21**, 1107–1110.

Ellis, M. A. & Dunlap, W. J. 1988. Displacement variation along thrust faults: implications for the development of large faults. *J. Struct. Geol.* **10**, 183–192.

Gawthorpe, R. L. & Hurst, J. M. 1993. Transfer zones in extensional basins: their structural style and influence on drainage development and stratigraphy. *J. geol. Soc. Lond.* **150**, 1137–1152.

Gilbert, C. M. 1938. Welded tuff in eastern California. *Bull. geol. Soc. Am.* **49**, 1829–1862.

Gillespie, P. A., Walsh, J. J. & Watterson, J. 1992. Limitations of dimension and displacement data from single faults and the consequences for data analysis and interpretation. *J. Struct. Geol.* **14**, 1157–1172.

Granier, T. 1985. Origin, damping and pattern of development of faults in granite. *Tectonics* **4**, 721–737.

Gudmundsson, A. 1992. Formation and growth of normal faults at the divergent plate boundary in Iceland. *Terra Res.* **4**, 464–471.

Izett, G. A. & Obradovich, J. D. 1994. $^{40}Ar/^{39}Ar$ age constraints for the Jaramillo normal subchron and the Mutuyama–Brunhes geomagnetic boundary. *J. geophys. Res.* **99**, 2925–2934.

Larsen, P.-H. 1988. Relay structures in a Lower Permian basement-involved extension system, East Greenland. *J. Struct. Geol.* **10**, 3–8.

Lubetkin, L. K. C. & Clark, M. M. 1988. Late Quaternary activity along the Lone Pine fault, eastern California. *Bull. geol. Soc. Am.* **100**, 755–766.

Marrett, R. & Allmendinger, R. W. 1991. Estimates of strain due to brittle faulting: sampling of fault populations. *J. Struct. Geol.* **13**, 735–738.

Martel, S. J., Pollard, D. D. & Segall, P. 1988. Development of simple strike-slip fault zones, Mount Abbot Quadrangle, Sierra Nevada, California. *Bull. geol. Soc. Am.* **100**, 1451–1465.

Peacock, D. C. P. 1991. Displacements and segment linkage in strike-slip fault zones. *J. Struct. Geol.* **13**, 1025–1035.

Peacock, D. C. P. & Sanderson, D. J. 1991. Displacements, segment linkage and relay ramps in normal fault zones. *J. Struct. Geol.* **13**, 721–733.

Peacock, D. C. P. & Sanderson, D. J. 1994. Geometry and development of relay ramps in normal fault systems. *Bull. Am. Ass. Petrol. Geol.* **78**, 147–165.

Pinter, N. 1992. Tectonic geomorphology and earthquake hazard of the northern Owens Valley, California. Unpublished Ph.D. thesis. University of California, Santa Barbara.

Savage, J. C., Lisowski, M., Prescott, W. H. & King, N. E. 1981. Strain accumulation near the epicenters of the 1978 Bishop and 1980 Mammoth Lakes, California, earthquakes. *Bull. seis. Soc. Am.* **71**, 465–476.

Segall, P. & Pollard, D. D. 1980. Mechanics of discontinuous faults. *J. geophys. Res.* **85**, 4337–4350.

Segall, P. & Pollard, D. D. 1983. Nucleation and growth of strike-slip faults in granite. *J. geophys. Res.* **88**, 555–568.

Sheridan, M. F. 1975. Tectonic displacement in the Bishop Tuff. *Calif. Geol.* **28**, 107–108.

Strand, R. G. 1967. Mariposa sheet. In: *Geologic Atlas of California.* Cal. Div. Mines and Geol. Scale: 1:250,000.

Trudgill, B. & Cartwright, J. 1994. Relay ramp forms and normal fault linkages, Canyonlands National Park, Utah. *Bull. geol. Soc. Am.* **106**, 1143–1157.

Walsh, J. J. & Watterson, J. 1988. Analysis of the relationship between displacement and dimensions of faults. *J. Struct. Geol.* **10**, 239–247.

Walsh, J. J. & Watterson, J. 1989. Displacement gradients on fault surfaces. *J. Struct. Geol.* **11**, 307–316.

Walsh, J. J. & Watterson, J. 1990. New methods of fault projection for coalmine planning. *Proc. Yorks. geol. Soc.* **48**, 209–219.

Walsh, J. J. & Watterson, J. 1991. Geometric and kinematic coherence and scale effects in normal fault systems. In: *The Geometry of Normal Faults* (edited by Roberts, A. M., Yielding, G. & Freeman, B.). *Spec. Publ. geol. Soc. Lond.* **56**, 193–203.

Watterson, J. 1986. Fault dimensions, displacements and growth. *Pure & Appl. Geophys.* **124**, 365–373.